Natural Resources Conservation and Research (2021) Volume 4 Issue 1
doi:10.24294/nrcr.v4i1.1551

ORIGINAL RESEARCH ARTICLE

Future forecast of global land wind and light resources in the context of climate change

Feimin Zhang[1], Chenghai Wang[1*], Guohui Xie[2], Weizheng Kong[2]

[1] College of Atmospheric Sciences, Lanzhou University, Key Laboratory for Arid Climatic Change and Disaster Reduction of Gansu Province, Lanzhou 730000, Gansu province, China. E-mail: wch@lzu.edu.cn*

[2] State Grid Energy Research Institute, Co., Ltd., Beijing 102209, China.

ABSTRACT

Based on the multi-model ensemble average results of the CMIP5 program, we predict the changes of global terrestrial wind and solar energy resources from 2020 to 2030 under different future climate change scenarios. The results show that the multi-mode ensemble average results have high confidence in the simulation of global wind and solar energy resources. Under different climate scenarios (RCPs), the changes in global terrestrial wind and solar energy resources in the next 2020–2030 (relative to 1986–2005) will have significant regional differences. Among them, wind resources in the Americas, Africa and Australia increased, while European wind-rich areas decreased; those in Asia (e.g., Northwest China and Central Asia) increased in RCP2.6, but decreased in RCP4.5 and RCP8.5. Global terrestrial solar energy resources are increasing in different RCPs scenarios in the future, especially in European solar energy-rich areas. Wind energy and solar energy resources on the global land have obvious seasonal variation characteristics, and the seasonal variation rate varies greatly in different regions. The change trend and change range of wind energy and solar energy resources in different rich areas are different. There are some differences in the RCPs scenario. It shows the complexity of future changes in wind and solar energy resources in response to global climate change.

Keywords: Wind and Solar Energy; Future Projection; Climate Change Scenario; CMIP Project

ARTICLE INFO

Received: 9 February 2021
Accepted: 12 March 2021
Available online: 19 March 2021

1. Introduction

In recent years, as an important part of clean energy, the utilization of wind and solar energy has developed rapidly around the world. The Global Wind Energy Commission (GWEC) forecast for the future global wind market suggesting that the global demand for renewable energy will gradually increase in the future and the wind market will grow steadily, especially in Asia, Europe and North America.

As the basic elements of renewable energy, near-stratigraphic wind speed and surface solar radiation have significant inter-chronological changes and regional differences. In recent years, the evaluation and estimation of renewable resources have become one of the hotspots of global attention[1-10]. Studies show that near-stratigraphic wind speeds decrease in most of the tropical and middle latitudes, while increasing in high latitudes[11,12]. In China, the daily average wind speed is greater than 3 $m \cdot s^{-1}$ decreases, and the overall wind speed shows a decreasing trend[13]. The change of wind energy is closely related to the east Asian monsoon circulation and under cushion surface[14]. The inter-decadal variation of surface solar radiation in China is characterized by an "ascending-descending" variation, and the overall trend is also decreas-

ing[15], which is mainly related to low cloud changes and human activities[16], while the solar radiation reaching the surface in Europe is on the increase, with an increase of about 5%[17].

With global climate change, the reserves and distribution of wind and solar energy resources will change accordingly in the future. The study concluded that, due to global warming, the average wind energy in the northern hemisphere mid-latitudes will decrease in the future, while the average wind energy in the tropics and southern hemisphere will increase[18]. In the 21st century, the annual mean wind speed at 10 m height in China tends to decrease in the high emission (A2), medium emission (A1B) and low emission (B1) scenarios, and the decreasing trend becomes more significant as the emission scenario increases[19]. Under the A2 emission scenario, the spatial distribution of wind energy resources in the 21st century is essentially the same as in the last 40 years of the 20th century, and the annual mean wind speed has a weakening trend in the first half of the 21st century, while an increasing trend dominates in the second half[20]. In the medium emission (A1B) scenario, the annual mean wind speed tends to increase over most of the United States, with a maximum increment of about 0.4 $m \cdot s^{-1}$[21]. Under the RCP4.5 and RCP8.5 emission scenarios, the wind speed increment in the South African region does not exceed 6%[22]. Under climate change scenarios, wind energy resources will increase in the future in north-central Europe (e.g., in and around the Baltic Sea), while they will decrease along the Mediterranean coast and in most of France, with insignificant interannual variability[23,24]. In the context of global warming, estimates of future solar energy resources indicate a 0% to 20% decrease in solar radiation on a seasonal scale in the continental United States[25]. In Japan, solar radiation will increase in the warm season and decrease in the cool season[26]. The overall solar radiation in central and southern Europe will increase by 5% to 10%, while the winter solar radiation in northern and eastern Europe will decrease by 5% to 15%[27]. Solar radiation in Nigeria will be reduced, especially in the southern part[28].

In summary, it can be seen that the near-surface wind speed and surface solar radiation as wind and light resources respond significantly to future climate change, but there are large uncertainties. The future changes of wind and light resources involve the development and utilization of global renewable resources, enterprise development, and resource construction layout. It is of great practical and scientific significance for national economic development to predict in advance the possible changes of future wind and solar resources in the context of climate change.

This paper attempts to use the simulation results of the international Coupled Mode Inter-comparison Project Phase 5 (CMIP5) to estimate the possible changes of global land wind and light elements from 2020 to 2030, and give the spatial and temporal change characteristics of wind and light resources, so as to provide scientific reference for the medium and long-term planning of the development and utilization of wind and light resources.

2. Materials and methods

Despite the large uncertainties in climate models, they are still the most reliable and indispensable tool to estimate the future climate change. The monthly data of air temperature, wind velocity and downward short-wave radiation in CMIP5 are used to study the future changes of global land wind velocity and solar radiation. In order to ensure model uniformity, 16 climate models including the above variables were selected from the historical test (RCP2.6, RCP4.5, RCP8.5) and the future tests with different typical emission concentration scenarios. Considering that the resolution of different climate models will have differences on the simulation results under the same emission scenario, a bilinear interpolation method is used to uniformly interpolate the results of all models to the bilinear interpolation method was used to uniformly interpolate all model results to a 2.5° × 2.5° grid point. For comparison, the period 1986–2005 is used as the current climate reference period, using the definition of the IPCC (Intergovernmental Panel on Climate Change) Working Group I Fifth Assessment Report (AR5, fifth assessment report).

There are few tests and assessment analyses on

the ability of GCMs to simulate near-surface wind speed and surface solar radiation, which are mainly limited by the large uncertainties in the model simulations of the two elements. Loew *et al*.[29] showed that the assessment results of CMIP models on a global scale rely heavily on the reanalysis of model information, and the simulation of interdecadal variability of solar radiation is subject to large errors and uncertainties. In this paper, eight models (**Table 1**) were selected for equal-weighted ensemble averaging to estimate the changes of global terrestrial wind and solar resources in 2020–2030 under different future climate scenarios (RPCs) based on the comparative analysis of the simulation capability of temperature and precipitation in the CRU (climate research units, version 4.01) reanalysis data for the same period. The global terrestrial wind and solar resources in 2020–2030 under different future climate scenarios (RPCs) are estimated relative to the historical reference period. It should be noted that the soundness of the above methods has been widely recognized in the field of climate change prediction, and the simulation capability of multi-model ensemble averaging is more reliable than that of a single model.

Table 1. Basic information of CMIP5 model for wind and light resource estimation

Model name	Country	Resolution	Points period	
			Historical experiments	Future prognostic tests
CanESM2	Canada	2.8° × 2.8°	1850–2005	2006–2100
MIROC5	Japan	2.8° × 2.8°	1850–2012	2006–2100
NorESM1-M	Norway	2.5° × 1.875°	1850–2005	2006–2100
IPSL-CM5A-LR	France	3.75° × 1.875°	1850–2005	2006–2300
IPSL-CM5A-MR	France	2.5° × 1.25°	1850–2005	2006–2100
HadGEM2-ES	United Kingdom	1.875° × 1.25°	1859–2005	2006–2299
HadGEM2-AO	Korea	1.875° × 1.25°	1859–2005	2006–2299
MRI-CGCM3	Japan	1.125° × 1.125°	1850–2005	2006–2100

Wind energy is the kinetic energy of air movement, which is the product of the wind turbine blade area, 3 times of wind speed and the air density. Wind energy per unit area of the wind turbine blade is defined as:

$$W = \frac{1}{2}\rho v^3 \tag{1}$$

Where: W is the wind energy per unit area of the wind turbine blade ($W \cdot m^{-2}$); ρ is the air density ($g \cdot m^{-3}$); v is the wind speed at the height of the wind turbine hub ($m \cdot s^{-1}$).

The above equation shows that wind energy is proportional to air density and wind speed, i.e., the greater the air density and wind speed, the greater the wind energy. However, air density has spatial variability. In order to eliminate the deviation of wind energy caused by spatial differences in density, a relationship between air density and altitude is established to make corrections based on the gas equation of state[30].

$$\rho_H = \rho_0 \left(1 - a\frac{H}{T_0}\right)^{4.26} \tag{2}$$

Where: ρ_H is the density of air at altitude H, ρ_0 is the density of air at room temperature and standard atmospheric pressure, taking the value of 1225 $g \cdot m^{-3}$ (the density of air at 15 °C at sea level); H is the altitude (m); T_0 is the absolute temperature (K), taking the value of 273 K; a is the decreasing rate of atmospheric vertical temperature, taking the value of 0.0065 $°C \cdot m^{-1}$.

The magnitude of solar energy depends mainly on the density of solar shortwave radiation flux (also known as irradiance, $W \cdot m^{-2}$) that reaches the ground. In general, the stronger the solar irradiance reaching the ground, the more abundant the solar energy.

The rate of change of global land-averaged wind and solar energy (R_{RCPs}) for 2020–2030 under different climate scenarios (RPCs) relative to the historical reference period (1986–2005) is calculated as follows:

$$R_{RCPs} = \frac{M_{RCPs} - M_{his}}{M_{his}} \tag{3}$$

Where: M_{RCPs} are the global terrestrial annual (seasonal) average wind and solar energy for different future climate scenarios; M_{his} is the global terrestrial annual (seasonal) average wind and solar

energy for the historical reference period.

2. Simulation capability of multi-model ensemble for global near-surface wind speed and solar irradiance

Figure 1 shows the global near-surface wind speed and solar irradiance distributions based on multi-model ensemble averaging. As seen in **Figure 1(a)**, there are significant regional differences in the global distribution of near-surface wind energy resources. The overall wind energy resources on the ocean are higher than on land, and the wind energy-rich areas on the ocean are mainly concentrated in the vast areas south of the equator near the poles, especially in the eastern hemisphere region, where the wind speed is above 7 $m \cdot s^{-1}$ in most of the sea. Onshore wind energy-rich areas are concentrated in North Africa, central North America, northwestern China, Central Asia and Australia, with relatively few wind energy resources at low latitudes near the equator. Compared with the global near-surface wind speed based on ground station observations released by NASA[31], the multi-model ensemble averaging results better reflect the approximate distribution of the actual global near-surface wind speed, but the simulated values are small, which may be related to the inconsistency between the simulated and observed altitudes of the near-surface wind speed.

From **Figure 1(b)**, it can be seen that global solar energy resources are mainly concentrated between the Tropic of Cancer near the equator, with solar irradiance usually above 200 $W \cdot m^{-2}$, and are most abundant in the Sahara region of northern Africa, while the eastern and southern parts of the African continent, Australia and northwestern China are also solar resource-rich areas. Compared with the solar irradiance observed by global ground-based weather stations published by NASA[31], the multi-model ensemble averaging results not only effectively reflect the approximate distribution of the actual global solar radiation, but also have a better reproducibility of the solar radiation magnitude values in different regions.

Comparing the multi-model ensemble averaging results with the observed spatial distribution of global near-surface wind speed and solar irradiance, the multi-model ensemble averaging results can reproduce the distribution and magnitude of global wind and solar energy resources better, which has high reliability. Therefore, this paper estimates the possible trend and distribution of wind and solar energy resources from 2020 to 2030 by using multi-model ensemble averaging results.

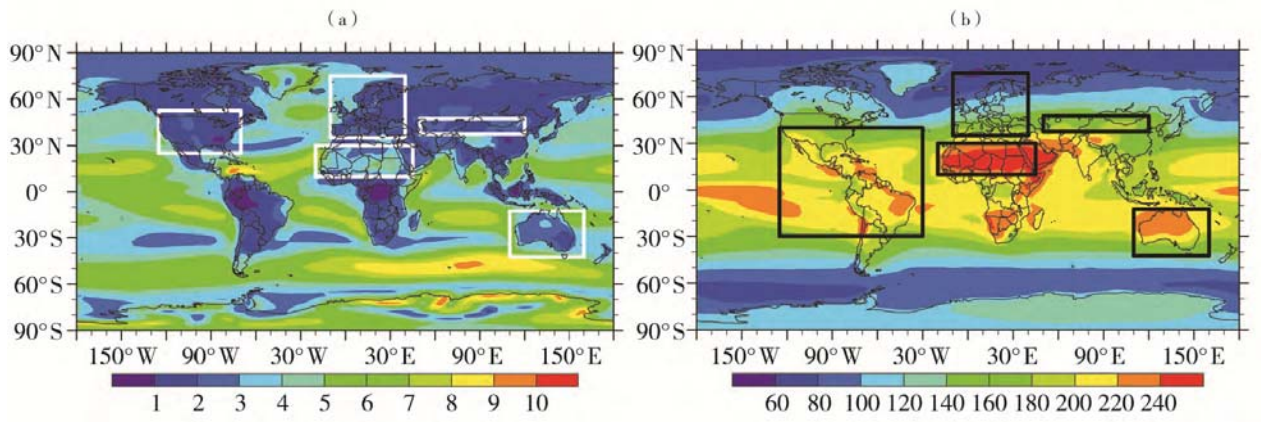

Figure 1. Multi-model ensemble-averaged global near-surface wind speed (**a**, unit: $m \cdot s^{-1}$) and surface solar irradiance (**b**, unit: $W \cdot m^{-2}$) distributions (high value areas are in the box).

3. Possible future changes in global terrestrial near-surface wind power density and solar irradiance

Figure 2 shows the annual rate of change distribution of global terrestrial near-surface wind and solar resources for the period 2020–2030 for different climate scenarios relative to the reference period (1986–2005). It can be seen that under different climate scenarios

(RCPs), the changes of global terrestrial wind energy resources from 2020 to 2030 are obviously spatial different. Under the RCP2.6 and RCP8.5 climate scenarios, compared with the period 1986–2005, most of the terrestrial wind energy resources show an increasing trend in 2020-2030, and some regions such as continental Antarctica, Greenland, western Canada, and Russia show a decreasing trend, and the wind-rich areas are mainly distributed in East Asia, Southeast Asia, northern and eastern China, Mongolia, Central Asia, 30°S–30°N region of America, northeastern Australia, and sub-Saharan Africa.

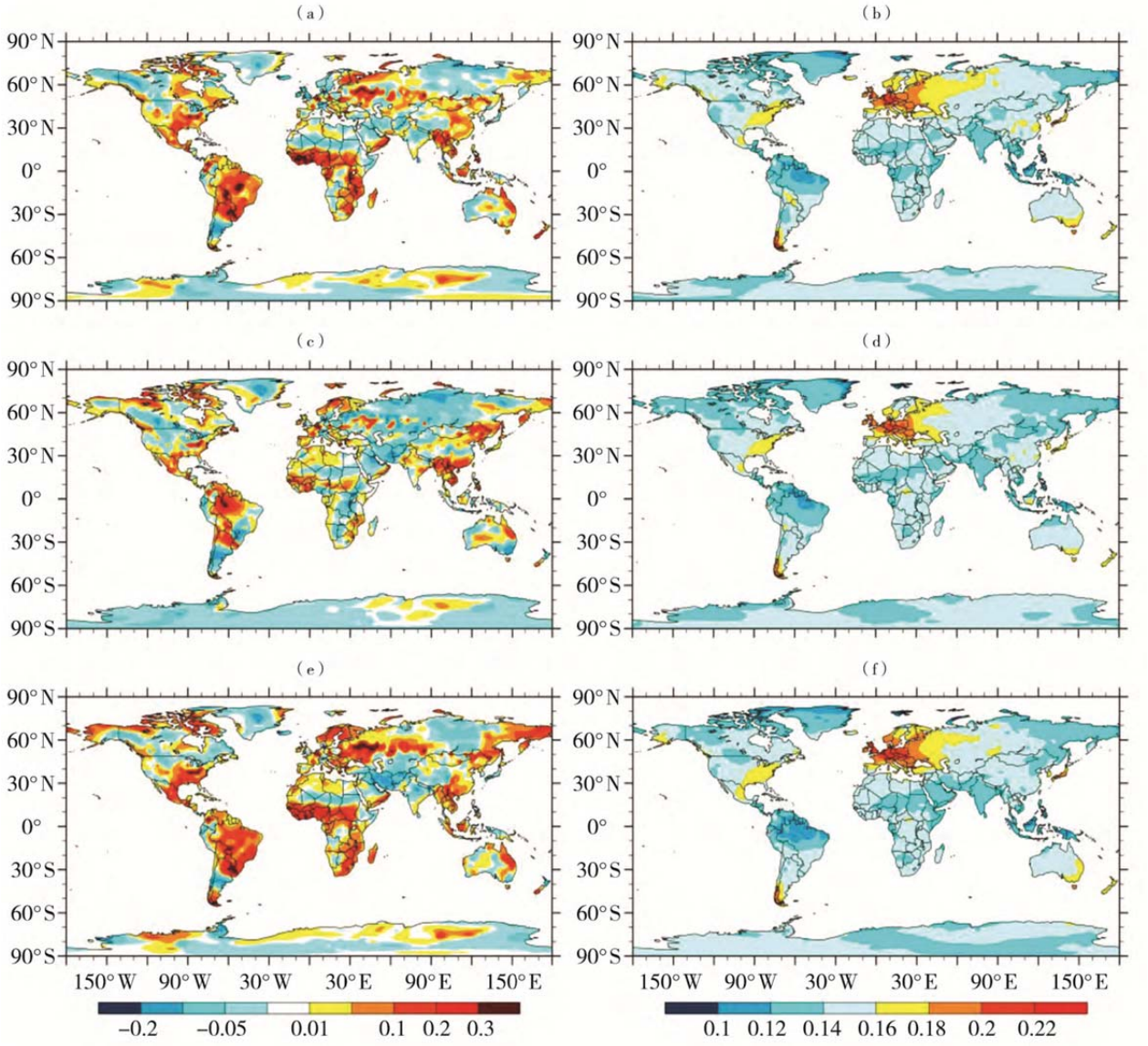

Figure 2. Rates of change in global land-averaged wind (**a**, **c**, **e**) and solar energy (**b**, **d**, **f**) for 2020–2030 under different climate scenarios (compared with the period from 1986 to 2005, the same as below). (**a**, **b**) RCP2.6, (**c**, **d**) RCP4.5, (**e**, **f**) RCP8.5.

At present, eastern China, Inner Mongolia, Hexi Corridor, Xinjiang and other regions are the places with the most abundant wind energy resources in China, in the past 10 a, the above areas have established large-scale wind power bases; under the RCP2.6 and RCP8.5 climate scenarios, these regions of China are still rich in future wind energy resources. Under the RCP4.5 scenario, the change distribution characteristics of wind energy resources from 2020 to 2030 are similar to that of RCP2.6 and RCP8.5 climate scenarios, but the increase range of wind energy resources is significantly reduced, and the increase range is relatively weak, among them, the European continent, Antarctica continent and most regions of Central Asia showed a decreasing trend. The spatial differences in the change of terrestrial wind energy resources from 2020 to 2030 under different RCPs scenarios may be related to

the change of polar climate and global sea and land thermal gradient in the context of global warming. The reasons still need to be further analyzed. Compared with the reference period, under different RCPs scenarios, the global solar energy resources increased between 2020 and 2030, and the most significant increase was in Europe, southeastern United States, southwest South America, and Southeast Australia, the increase in solar resources in these regions was most pronounced under the RCP8.5 climate scenario, indicating a significant increase trend in solar resources between 2020 and 2030 under the high emission scenario. This may be related to the future reduction in cloud volume for reasons that need further investigation.

According to the NASA global near-surface wind speed and solar radiation observation material[31] and multi-mode ensemble averaging results (**Figure 1**), the onshore wind and solar-rich areas are mainly concentrated in the Americas, the Sahara region in Africa, Australia, Europe, Northwest China and Central Asia. Therefore, for the above five regions, this paper further discusses the characteristics of wind energy, solar energy resources annually and seasonal changes under different climate scenarios. January, April, July and October were selected to represent winter, spring, summer and autumn, respectively.

Figure 3 shows the annual and seasonal average percent change in global terrestrial wind and solar resources for 2020–2030 under different RCPs climate scenarios relative to the reference period. It can be seen that there are significant seasonal differences in global terrestrial wind and solar energy resources under different future climate scenarios, and the response to different RCPs varies greatly.

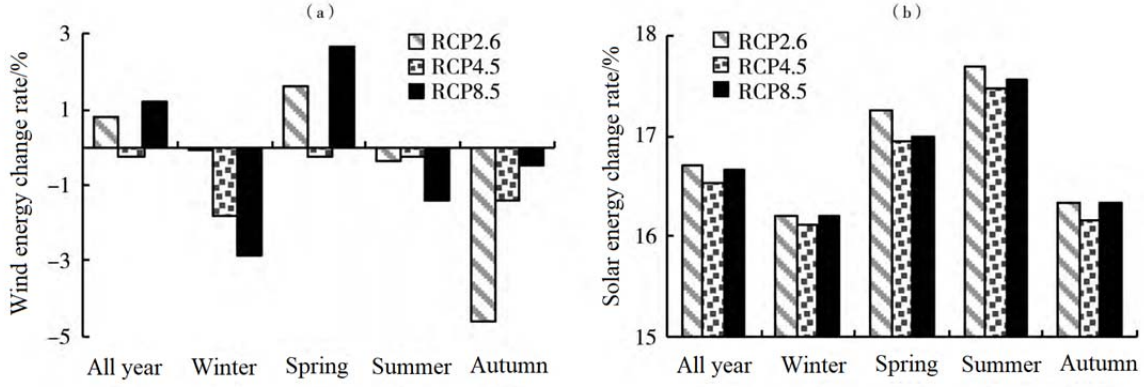

Figure 3. Annual and seasonal average rates of change in global land-based wind (**a**) and solar (**b**) resources for 2020–2030 under different climate scenarios.

From **Figure 3(a)**, it can be seen that relative to the reference period (1986–2005), the global land-based annual average wind resource increases during the period 2020–2030 under the RCP2.6 and RCP8.5 climate scenarios, and increases more significantly under the RCP8.5 scenario than the RCP2.6 scenario, while decreases under the RCP4.5 scenario, but the trend varies from season to season. Among them, the land average wind energy resources in winter, summer and autumn all decreased under different RCPs (except for the winter RCP2.6 scenario), wind energy resources in winter and summer are most significantly in the RCP8.5 scenario, in autumn, the wind energy resources decreased most significantly in the RCP2.6 scenario; the change trend of wind energy resources in spring is consistent with the whole year, in a slight reduction in the RCP4.5 climate scenario, while the increase is significant in the RCP2.6 and RCP8.5 scenarios, and the rate of increase is higher than the annual average. It can be seen that under the future high and low emission scenarios, the onshore wind energy resources show a general decreasing trend during the period 2020–2030, except for a significant increase in spring.

As seen in **Figure 3(b)**, the global terrestrial annual and seasonal average solar resources increase from 2020 to 2030 relative to the reference period, and the increase is most pronounced in the RCP2.6 and RCP8.5 scenarios, with the largest increase in summer.

To sum up, compared with the reference period,

the changes in the global terrestrial average wind and solar resources between 2020 and 2030 did not increase or decrease with the increasing RCP emission concentration, indicating that future changes in wind and solar resources are nonlinear in response to climate change.

Table 2 statistics the annual and seasonal average change rates of wind and solar energy resources over the reference period from 2020 to 2030 for different RCPs. It can be seen that the annual average wind energy resources in the rich regions of America, Africa and Australia show an increasing trend under different climate scenarios, and the increasing trend is most pronounced in the rich regions of Africa. The annual mean wind resource variability in the Asian rich region (Northwest China and Central Asia, hereafter) is relatively complex, with an increasing trend under the RCP2.6 scenario and decreasing trends under the RCP4.5 and RCP8.5 scenarios. In different seasons, wind energy resources in the rich regions of the Americas and Africa in winter show consistent decreasing and increasing trends under different climate change scenarios; The wind resource in the Asian rich region tends to increase under the RCP2.6 scenario and decrease under the RCP4.5 and RCP8.5 scenarios, with the most significant decrease in the RCP4.5 scenario. Wind resources in Australia and the European rich zone decrease under the RCP4.5 scenario and increase under the RCP2.6 and RCP8.5 scenarios. In spring, the wind energy resources showed a consistent increasing trend across climate change scenarios, except in the African rich zone, where the trend varied across climate change scenarios. In particular, wind energy resources in the Asian rich region show a decreasing trend under the RCP2.6 scenario and an increasing trend under the RCP4.5 and RCP8.5 scenarios, which is the opposite of the winter season. In summer, wind energy resources in the Americas, Africa and Europe increase under different climate change scenarios, wind energy resources in Asian rich region are decreasing under different climate change scenarios, and the reduction is the most obvious in the RCP4.5 scenario, but the changing trends of Australia's rich regions are different. In autumn, wind energy resources in rich areas of the Americas and Australia increase under different climate change scenarios; Wind energy resources in the rich regions of Asia increased in the RCP2.6 and RCP8.5 scenarios, but decreased in the RCP4.5 scenario.

According to the above analysis, the wind energy resources in the five major rich regions of the world, except for Europe and Asia, will generally show an increasing trend from 2020 to 2030 under different climate scenarios in the future. In addition, global terrestrial wind energy resources are significantly seasonal and regional under different climate change scenarios, indicating that wind energy resources in different seasons and regions have different responses to different climate change scenarios.

Table 2. Annual and seasonal average rates of change of wind and solar energy resources in different parts of the global land under different climate scenarios, relative to the reference period 2020–2030

Enrichment area	Future climate scenarios	Wind energy					Solar energy				
		Winter	Spring	Summer	Autumn	All year	Winter	Spring	Summer	Autumn	All year
Americas	RCP2.6	-10.8	0.99	17.79	3.02	3.02	15.97	16.28	15.62	16.40	16.08
	RCP4.5	-0.63	-10.68	14.52	11.35	0.25	15.94	15.82	16.08	16.11	16.20
	RCP8.5	-5.93	-2.94	20.45	6.18	3.16	15.62	15.87	15.91	16.17	16.10
Africa	RCP2.6	0.87	5.43	3.17	1.2	3.33	16.68	16.61	16.92	15.84	16.85
	RCP4.5	0.58	8.01	3.21	-1.96	3.22	16.75	17.01	16.60	16.61	17.05
	RCP8.5	3.51	7.89	1.95	-1.89	3.32	16.71	16.68	16.53	15.56	16.67
Asia	RCP2.6	0.43	-1.09	-1.11	3.52	0.63	16.10	17.00	18.34	17.17	17.54
	RCP4.5	-1.82	1.59	-5.00	-5.34	-0.98	15.20	16.39	18.08	16.35	17.20
	RCP8.5	-0.17	1.84	-0.28	4.36	-0.48	16.32	16.70	18.74	17.08	17.58
Australia	RCP2.6	3.10	2.38	3.00	12.10	3.11	17.98	17.33	18.41	17.64	17.66
	RCP4.5	-6.96	1.12	-1.02	10.00	1.24	17.11	17.23	18.00	16.85	17.06
	RCP8.5	4.36	-9.14	5.80	6.98	2.08	17.10	18.04	18.19	17.54	17.22
Europe	RCP2.6	4.33	-1.14	2.43	0.51	-0.29	15.88	17.74	18.23	17.04	18.00
	RCP4.5	-0.95	-1.22	2.39	-2.72	-1.86	15.47	17.24	17.83	16.15	17.46
	RCP8.5	0.55	1.89	3.22	-0.13	-0.03	15.97	17.35	17.95	16.68	17.82

According to the annual and seasonal average rate of change of solar energy resources from the five major global land rich regions in the 2020–2030 which relative to the reference period (**Table 2**), solar energy resources in different regions show an increasing trend in different climate change scenarios and different seasons, that is, solar energy resources in the rich areas of the global land always show an increasing trend in the future climate change scenarios.

In terms of annual averages, solar resources in the global continent-rich regions increase most significantly in Europe under different climate change scenarios in 2020–2030, followed by Asia and Australia, with relatively small increases in solar resources in the Americas and Africa.

Under different climate change scenarios, the increase in solar energy resources is most pronounced in winter in the Australian-rich region and least in the European-rich region. In spring, the most significant increases in solar resources were seen in Australia and Europe, with relatively small increases in other regions; in summer and fall, the most significant increases were seen in Asia, Australia and Europe, with relatively small increases in the Americas and Africa. Among them, the solar energy resources in the Asian-rich regions increased the most significantly under the RCP8.5 scenario. It can be seen that there are also significant regional and seasonal differences in the increase of global terrestrial solar resources in 2020–2030 under different climate change scenarios. It should be noted that under future climate change scenarios, wind energy resources vary significantly more than solar energy resources across seasons, which is related to the strong transient and volatile nature of wind speed itself (small spatial and temporal scales)[2].

4. Conclusion and discussion

(1) The multi-model ensemble averaging results based on the CMIP5 program can better reproduce the global near-surface wind speed and the distribution of surface solar short-wave radiation, and the simulation performance for solar radiation is better. It shows that the multi-model ensemble averaging results have high confidence in the simulation of wind and solar resources on a global scale.

(2) Compared with the reference period, the changes of global terrestrial wind and solar energy resources between 2020 and 2030 under different RCPs scenarios have obvious regional differences. The regional difference of solar energy resources was small. Each rich area showed an increasing trend under different RCPs, and showed the most obvious increasing trend under the high emission (RCP8.5) scenario. The regional variation of wind energy resources is great, and the change trend of different rich areas under different RCPs is also quite different.

(3) Compared with the reference period, there are still obvious seasonal differences in wind and solar energy resources in different regions of the world between 2020 and 2030 under different climate scenarios, and the seasonal differences of wind energy resources are stronger than those of solar energy resources. The changes in wind and solar energy resources from 2020 to 2030 did not increase or decrease with the increasing emission concentration, indicating the complexity and nonlinearity of future wind and solar energy resource responses to global climate change.

It should be noted that although the climate system model has been continuously improved in the past decade and the simulation capacity has gradually improved, the model still has great uncertainty, also reflected in the simulation of near-surface wind speed and surface solar radiation[32]. Moreover, the climate model has a “climate drift” phenomenon in the long integration process, which manifests itself as spurious changes independent of internal variability or external forcing[33,34].It has been shown that the near-surface wind speeds from GCM results and reanalysis data differ significantly at high altitudes, especially north of 30°N, where the correlation coefficients between the two are low[35]. Among them, the GCM simulation of near-surface wind speed in China is small[36].

The mechanisms of wind and solar resource changes in the context of climate change are more complex, and atmospheric circulation, ENSO (El Niño-Southern Oscillation), topographic thermodynamic effects, subsurface changes, and anthropogenic effects all have an impact on the changes of wind speed in the global terrestrial near-surface

layer, but the corresponding explanations of the mechanisms still differ greatly[37-40]. Therefore, with the continuous improvement and development of the model, the predicted results of wind and solar resources will be more credible in the future.

Conflict of interest

The authors declared that they have no conflict of interest.

Reference

1. Wang C, Liu C. Woguo fengdian jianshe zhong fengziyuan pinggu cunzai de wenti he yingduicuoshi (Chinese) [Problems and countermeasures existing in the stroke resource evaluation of wind power construction in China]. Proceedings of the CSEE 2011; 31(Suppl.): 242–245.
2. Zhang F, Wang C. The application of observation data assimilating in wind power prediction. 2nd International Conference on Applied Robotics for the Power Industry (CARPI); 2012 Sep 11–13; Zurich, Switzerland. New York: IEEE; 2012. p. 137–139.
3. Zhang F, Yang Y, Wang C. The effects of assimilating conventional and ATOVS data on forecasted near-surface wind with WRF-3DVAR. Monthly Weather Review 2015; 143(1): 153–164.
4. Wang C, Jin S. Error features and their possible causes in simulated low-level winds by WRF at a wind farm. Wind Energy 2014; 17(9): 1315–1325.
5. Wang C, Jin S, Hu J, *et al*. Comparing different boundary layer schemes of WRF by simulation the low-level wind over complex terrain. 2011 2nd International Conference on Artificial Intelligence, Management Science and Electronic Commerce (AIMSEC); 2011 Aug 8–10; Zhengzhou, China. New York: IEEE; 2011. p. 6183–6188.
6. Zhang F, Wang C. Experiment of surface-layer wind forecast improvement by assimilating conventional data with WRF-3DVAR. Plateau Meteorology 2014; 33(3): 675–685.
7. Xing T, Zheng Y, Zhu Y. Research on the development and exploitation of wind energy resources in Yunnan Province. Meteorological and Environmental Sciences 2013; 36(4): 55–61.
8. Fei Y, Xia X. Decadal variations of aerosol-cloud-radiation in Eastern China and their relationships during 1980–2009. Meteorological and Environmental Sciences 2016; 39(2): 1–9.
9. Zhu X, Li H. Analysis and evaluation of solar energy resources in Luoyang area. Meteorological and Environmental Sciences 2015; 38(1): 67–72.
10. Si F. Assessment analysis of solar radiation resources in Jiaozuo. Meteorological and Environmental Sciences 2013; 36(2): 87–91.
11. Vautard R, Cattiaux J, Yiou P, *et al*. Northern hemisphere atmospheric stilling partly attributed to an increase in surface roughness. Nature Geoscience 2010; 3(11): 756–761.
12. Mcvicar TR, Roderick ML, Donohue RJ, *et al*. Global review and synthesis of trends in observed terrestrial near-surface wind speeds: Implications for evaporation. Journal of Hydrology 2012; 416: 182–205.
13. Jiang Y, Luo Y, Zhao Z. Jin wushi nian zhongguo fengsu bianhua ji yuanyin fenxi (Chinese) [Analysis of wind speed changes and causes in China in the last 50 years]. Proceedings of the 24th Annual Meeting of the Chinese Meteorological Society; 2007 Oct 13–16; Qingdao. Beijing: Chinese Meteorological Society; 2007.
14. Zhang T, Yan J, Li S, *et al*. Influence of climate change on wind energy resources in agriculture and stock-raising interlaced region of Northern China. Journal of Arid Meteorology 2012; 30(2): 202–206.
15. Wang C, Zhang Z, Tian W. Factors affecting the sur-face radiation trends over China between 1960 and 2000. Atmospheric Environment 2011; 45: 2379–2385.
16. Ma J, Luo Y, Shen Y, *et al*. Regional long-term trend of ground solar radiation in China over the past 50 years. Science China: Earth Sciences 2012; 42(10): 1597–1608.
17. Turnock ST, Spracklen DV, Carslaw KS, *et al*. Modelled and observed changes in aerosols and surface solar radiation over Europe between 1960 and 2009. Atmospheric Chemistry and Physics 2015; 15(9): 13457–13513.
18. Karnauskas KB, Lundquist JK, Zhang L. Southward shift of the global wind energy resource under high carbon dioxide emissions. Nature Geoscience 2018; 11(1): 38–43.
19. Jiang Y, Luo Y, Zhao Z. Projection of wind speed changes in China in the 21st century by climate models. Chinese Journal of Atmospheric Sciences 2010; 34(2): 323–336.
20. Li Y, Tang J, Wang Y, *et al*. Prediction of climate change of the near-surface wind energy potential over China. Acta Energiae Solaris Sinica 2011; 32(3): 338–345.
21. Liu B, Costak B, Xie L, *et al*. Dynamical downscaling of climate change impacts on wind energy resources in the contiguous United States by using a limited-area model with scale-selective data assimilation. Advances in Meteorology 2014; 2014: 1–11.
22. Herbst L, Rautenback H. Climate change impacts on South African wind energy resources. Africa Insight 2016; 45: 1–31.
23. Carvalho D, Rocha A, Gomez-Gesteira M, *et al*. Potential impacts of climate change on European wind energy resource under the CMIP5 future climate projections. Renewable Energy 2017; 101: 29–40.
24. Najac J, Lac C, Terray L. Impact of climate change on surface winds in France using a statistical-dynamical downscaling method with mesoscale modelling. International Journal of Climatology 2011; 31: 415–430.

25. Pan Z, Christensen JH, Arritt RW, *et al*. Evaluation of uncertainties in regional climate change simulations. Journal of Geophysical Research: Atmospheres 2001; 106: 17735–17751.
26. Iizumi T, Nishimori M, Yokozawa M. Combined equations for estimating global solar radiation: Projection of radiation field over Japan under global warming conditions by statistical downscaling. Journal of Agricultural Meteorology 2008; 64: 9–23.
27. Ruostenja K, Raisanen P. Seasonal changes in solar radiation and relative humidity in Europe in response to global warming. Journal of Climate 2013; 26: 2467–2481.
28. Ohunakin OS, Adaramola MS, Oyewola OM, *et al*. The effect of climate change on solar radiation in Nigeria. Solar Energy 2015; 116: 272–286.
29. Loew A, Anderson A, Trentmann J, *et al*. Assessing surface solar radiation fluxes in the CMIP ensembles. Journal of Climate 2016; 29(20): 7231–7246.
30. Bai S, Lu J. Analysis on influence of Tibet High Plateau climate on wind power generation. Electric Power Construction 2006, 27(11): 37–40.
31. Nema P, Nema RK, Rangnekar S. A current and future state of art development of hybrid energy system using wind and PV-solar: A review. Renewable and Sustainable Energy Reviews 2009; 13(8): 2096–2103.
32. Knutti R, Sedláček J. Robustness and uncertainties in the new CMIP5 climate model projections. Nature Climate Change 2013; 3(4): 369–373.
33. Dirmeyer PA. Climate drift in a coupled land atmosphere model. Journal of Hydrometeorology 2009; 2(1): 89–102.
34. Gupta AS, Muir LC, Brown JN, *et al*. Climate drift in the CMIP3 models. Journal of Climate 2012; 25(13): 4621–4640.
35. Mcinnes KL, Erwin TA, Bathols JM. Global climate model projected changes in 10 m wind speed and direction due to anthropogenic climate change. Atmospheric Science Letters 2011; 12(4): 325–333.
36. Jiang Y. Zhongguo feng he fengneng bianhua yanjiu (Chinese) [Study on wind and wind energy change in China] [PhD thesis]. Nanjing: Nanjing University of Information Science and Technology; 2009. p. 1–192.
37. Li Y, Wang Y, Chu H, *et al*. Zhongguo luyu jindiceng fengneng ziyuan de qihou bianyi he xiadianmian ren wei gaibian de yingxiang (Chinese) [Effects of climate variability and anthropogenic modification of subsurface on near-surface wind energy resources in China's land area]. Chinese Science Bulletin 2008, 53(21): 2646–2653.
38. Zhao Z, Luo Y, Jiang Y. Is global strong wind decling? Advances in Climate Change Research 2011; 7(2): 149–151.
39. Li X, Zhong S, Bian X, *et al*. Climate and climate variability of the wind power resources in the Great Lakes region of the United States. Journal of Geophysical Research: Atmospheres 2010; 115(D18).
40. Berg N, Hall A, Capps SB, *et al*. El Niño-Southern oscillation impacts on winter winds over Southern California. Climate Dynamics 2013; 40(1): 109–121.